

E. STODOLAK-ZYCH<sup>1\*</sup>, M. KUDZIN<sup>2</sup>, K. KORNAUS<sup>1</sup>, M. GUBERNAT<sup>1</sup>,  
E. KANIUK<sup>1</sup>, M. BOGUN<sup>2</sup>

## NONWOVEN CARBON FIBERS WITH NANOMETRIC METALLIC LAYERS AS A TOOL TO MONITOR REGENERATIVE PROCESSES

Still unsolved is the problem of monitoring the tissue regeneration with the use of implants (substrates) in *in vivo* conditions. The multitude of implant materials combined with their specific immanent often limit standard diagnostic methods, i.e. X-ray or computer tomography (CT). This is particularly difficult in therapies using polymeric high-resistance substrates for tissue engineering. The aim of this study was to fabricate a non-woven carbon fiber composed of carbon fibers (CF) which were then subjected to a surface modification by magnetron sputtering. A layer of iron (Fe) was applied under inert conditions (argon) for different time periods (2-10 min). It was shown that already after 2-4 minutes of iron sputtering, the voxel surface (CF\_Fe2', CF\_Fe4') was covered with a heterogeneous iron layer observed by scanning electron microscope (SEM) with energy dispersive X-ray analysis (EDS). The longer the modification time, the more uniform the layer on the fiber surface becomes. This can be seen by the change in the wettability of the nonwoven surface which decreases from 131° for CF\_Fe2 to 120° for CF\_Fe10. The fibers do not change their geometry or dimensions (~11.5 μm). The determination of pore size distribution by adsorption and desorption techniques (BJH) and specific surface area by nitrogen adsorption method (BET) have shown that the high specific surface area for the CF\_Fe2' fibers decreases by 10% with the increasing iron sputtering time. All the studied CF\_Fe fibers show good biocompatibility with osteoblast-like cells MG-63 cells after both 3 and 7 days of culture. Osteoblasts adhere to the fiber surface and show correct morphology.

*Keywords:* Activated carbon fibers; nanometric layers; magnetron sputtering; cells-materials interaction

### 1. Introduction

Micrometric carbon fibers with an active surface (ACF) are materials used both in environmental protection (pollutant absorbents) and medicine [1]. Compared with traditional granular activated carbon, they have a smaller fiber diameter and a more concentrated pore distribution, a larger specific surface area, faster adsorption kinetics, and a bigger adsorption capacity. Activated carbon fibers (ACF) can be prepared from various precursors such as: synthetic polymers (ie. polyacrylonitrile PAN, cellulose acetate, CA), biopolymers (cotton, cellulose) and other materials, e.g. coal, rayon, phenolic resins and pitches [2]. Depending on the precursor used to obtain ACF but also on the activation conditions (temperature, activation time, special methods of surface modification ie.: PCV, CVD), the final fibrous materials differ significantly in texture and sorption properties [3,4]. The most common carbon fibers precursor used to obtain ACF is polyacrylonitrile (PAN). This polymer precursor

needs a two-step thermal treatment: oxidation and carbonization to convert a polymer structure to a carbon structure. It shows the excellent adsorption performance because of its nano-structure, abundant micrometer porosity, high specific surface area and narrow pore size distribution [5]. These textural parameters can be still improved by chemical (phosphoric acid, ammonia, nitric acid, potassium hydroxide, and ammonium persulfate), thermal or physical treatment (PVD, CVD method) [6-8]. Non-woven fabrics composed of micrometric fibers can be used as membranes or scaffolds for tissue regeneration thanks to their specific surface enabling particular and selective interaction with biological molecules and cells [9]. Carbon fibers in the form of nonwoven fabrics are used in biomedical engineering as biomimetic substrates to fill bone or cartilage tissue defects. Unfortunately, there is a problem with monitoring the process of tissue self-repair. Available diagnostic techniques, such as X-ray, CT or MRI, do not always work well for cartilaginous defects. The low density of the implant relative to the surrounding tissue

<sup>1</sup> AGH UNIVERSITY OF SCIENCE AND TECHNOLOGY, DEPARTMENT BIOMATERIALS AND COMPOSITES, AL. MICKIEWICZA 30, 30-059 KRAKOW, POLAND

<sup>2</sup> LUKASIEWICZ – LODZ INSTITUTE OF TECHNOLOGY, LODZ, POLAND

\* Corresponding author: [stodolak@agh.edu.pl](mailto:stodolak@agh.edu.pl)



(in CT) or total transparency to radiation (in X-ray) or the lack of a contrast agent (in MRI) make it difficult to track the defect regeneration. An alternative approach may be using activated carbon fibers to support a marker facilitating the visualization of the MRI technique. ACFs have a high specific surface area and high electrical conductivity, which enables the iron film deposition process by methods based on physical vapor deposition (PVD). Magnetron sputtering is one of the methods in the PVD family that modifies a surface by coating it with a film or coating [10]. Iron particles are deposited on the fibrous substrate so the morphology of the fiber surface plays an important role.

In our research we used classical low modulus carbon fibers dedicated for biomedical application, subjected to appropriate physicochemical treatment, i.e. magnetron sputtering, and enriched in a nanometric layer of iron (Fe). The presence of a nanometric iron layer can help to monitor tissue regeneration using magnetic resonance imaging (MRI). The samples were modified using the magnetron sputtering system with metallic layers deposited in different time periods (from 1 to 10 min). The effect of the layer on physicochemical properties, such as specific surface area, contact angle and porosity, was evaluated. A biocompatibility test was performed by contacting cells with the scaffold.

## 2. Materials and methods

Carbon fibers were prepared by the two-step thermal conversion of a polymer precursor according to a procedure described previously [11]. The oxidation validity and carbonization process were verified by determining the material shrinkage after each step and the structural changes typical of the thermal conversion process (FTIR). The carbon fibers were modified by magnetron sputtering for different time period using the optimal chamber conditions (TABLE 1). The surface morphologies of the carbon fibers and the iron-modified fibers were observed using scanning electron microscopy (SEM, Nova NANOSEM). The fibers cross-sections were also obtained to determine the surface areas and the aspect ratio (TABLE 2). The fibre diameter was determined from microscopic images using ImageJ software. Layer thickness was estimated using SEM microscope software that allowed measurement of the cross-sectional diameters of pristine and modified fibers. By comparing the diameters, it was possible to estimate the value of the layer thickness. Complimentary research was made for areas where the metallic layer was discontinuous, and layer thickness was measured there. The method of modification of the surface of fiber with a circular geometry does not allow to obtain a homogeneous and continuous layer an estimated value of the layer thickness is given, without assigning it to the iron deposition times (Fig. 2). The total porosity and pore size (inter-fibers area) were measured by means of mercury porosimetry (PoreMaster 60, Quantachrome Instruments, USA). Also, the specific surface area of the fibers with and without the iron layer was determined using the BET method (TABLE 2).

TABLE 1

Parameters of magnetron sputtering processes for carbon substrates (CF)

Samples	Time sputtering, min	Chamber's atmosphere	Working pressure, hPa	Effective power, kW
CF_Fe2'	2	argon (4%)	$2,9 \cdot 10^{-3}$	1
CF_Fe4'	4			
CF_Fe6'	6			
CF_Fe8'	8			
CF_Fe10'	10			

The fibrous substrates were contacted with osteoblast-like MG-63 cells (European Collection of Cell Cultures, Salisbury, UK), and the cell morphology and functional state were observed during the live-dead stain test. Before staining, the culture was washed with 1 ml PBS, then the mixtures of dyes, i.e. propidium iodide (PI) and calcian AM in a 1:1 ratio, both at a concentration of 1 mg/ml (Sigma Aldrich, Germany) were added. The biological studies were carried out using osteoblast-like cells MG-63 (ATCC). The cells were stored in an incubator under conditions of 5% CO<sub>2</sub> and 37°C until formation of a confluent layer and then passaged through scraping (5 times). Prior to the test, all the samples were cut into 12 mm discs (6 discs for viability tests and 6 discs for cytotoxicity tests after 3 and 7 days – a total of 32 samples per variant), sterilized by UV irradiation. Then the cells were diluted to obtain 10 000 cells/ml (counted using the Bürker's hemocytometer) and added to the samples containing discs. For both tests (viability and cytotoxicity) the tissue culture polystyrene (TCPS) discs were used as a control material and an CF substrate as a reference sample. The cell viability was determined by the Vialight®Plus assay (BioAssay Kit, Lonza, Basel, Switzerland) considered complementary to the cytotoxicity assay (Toxilight) [12,13].

## 3. Results and discussion

Time is used as a variable to limit the impact of various application process parameters affecting the quality of the layer (i.e. working gas pressure, operating power and target-substrate distance). Thus, the analysis of further results allows a comparative approach to materials differing only in the amount of iron (layer thickness) on the surface of carbon fibers [10]. The initial carbon fibers are characterized by a smooth and homogeneous surface and a diameter of  $11.57 \pm 1.23 \mu\text{m}$  (Fig. 1a). The iron layer causes a change in both the morphology and the fiber diameter size. After 2 minutes of iron sputtering, the fibers become rough and their diameter is reduced to a value of  $11.36 \pm 1.22 \mu\text{m}$ . This allows us to conclude that during the process of iron bombardment in a protective atmosphere, the fibrous surface disintegrates. As a result, furrows and irregularities are formed on the surface and the fiber diameter is reduced (Fig. 1b). The prolonged deposition time results in an increase in the fiber diameter (up to  $11.96 \mu\text{m}$  for CF\_Fe10') with the surface smoothed to a slight degree (Fig. 1f).

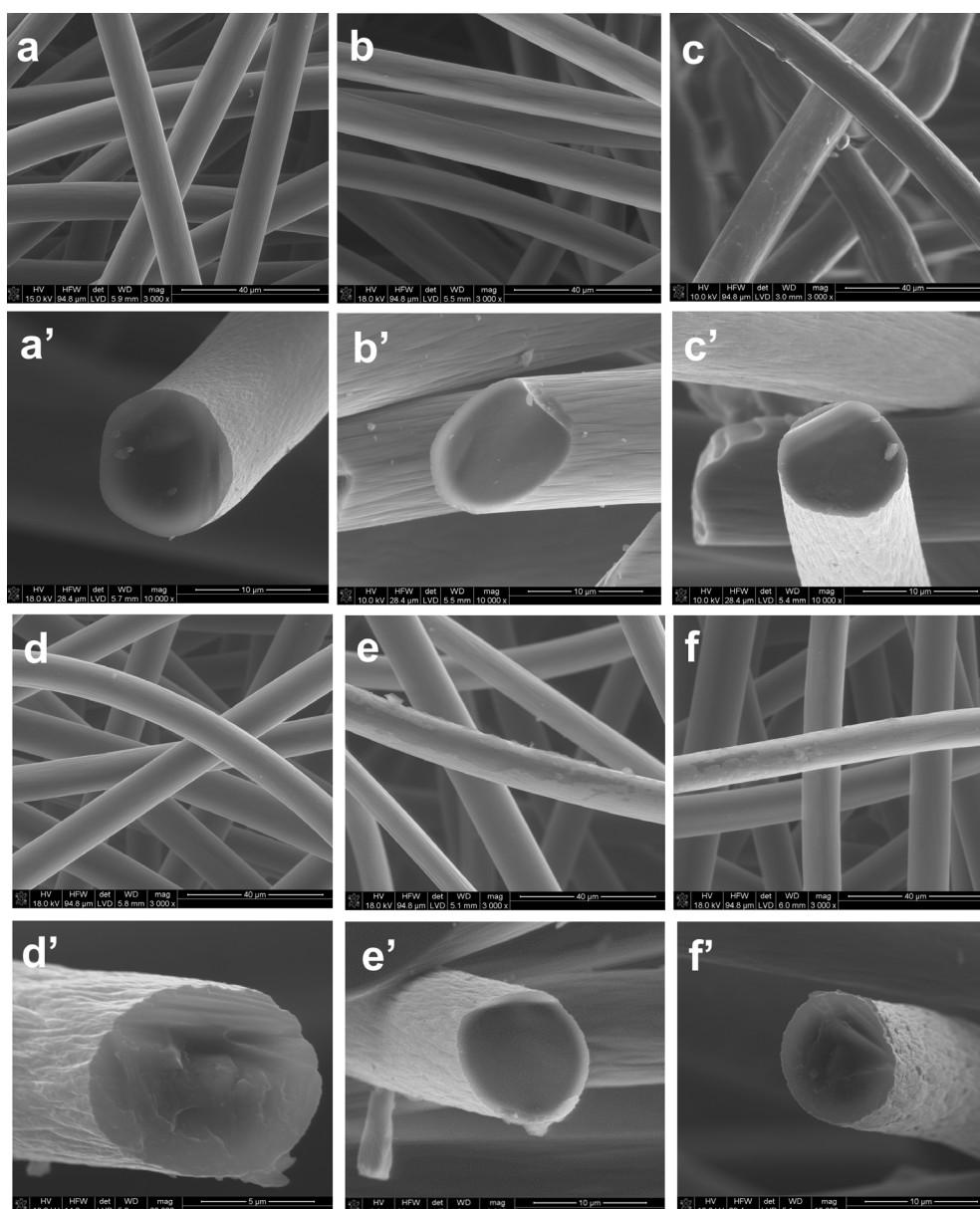


Fig. 1. Morphology of reference carbon fibres CF and their cross-section (a,a'). Morphology of the surface of carbon fibers with an iron layer applied CF\_Fe and their cross-section after 2 min (b, b'), 4 min (c, c'), 6min (d, d'), 8 min (e, e') and 10 min (f, f')

The amorphous carbon is removed from the fiber surface, resulting in a change in the pore structure and its unevenness. Some authors report that increasing the time of thermal, chemical or other modification can lead enlargement of micropores, thus reducing the fibers absorption capacity [14,15]. The changes occurring on the surface of carbon fibers during the activation process should be under special supervision in the case of activated carbon fibers. Uncontrolled processes on the ACF surface disqualify the material from the planned use [16].

In all iron-modified fiber materials, the presence of this element was confirmed by the EDS analysis (Fig. 2). It was noted that the deposition time longer than 8 minutes results in an inhomogeneous and thicker iron layer. The images show cracks in the layer (Fig. 1e-f). This is a factor that prevents the use of this material in clinical applications, where the amount of iron and its location must be under control [17].

On the basis of the microscopic analysis, it was found that taking into account the fiber shape and size before and after the modification, it can be concluded that the surfacing causes a change in the fiber surface, while the fiber aspect ratio does not change. The fibers after the iron modification change their diameter, which depends on the evaporation time and thus on the iron layer thickness (TABLE 2). The presence of iron affects the fibers wettability which decreases relatively to the initial nonwoven ones (Fig. 3). This is a synergistic effect resulting from both the smoothing of the fiber surface and from the changing surface chemistry of the iron-coated fiber. The longer the evaporation time, the lower the wettability (for CF\_Fe10' it is about 120°, while for CF\_Fe2' it is 15 degrees higher and amounts to about 135°). The modification of ACF surfaces has one purpose – to increase their attractiveness for subsequent applications [17,18]. It seems that in the case of magnetron

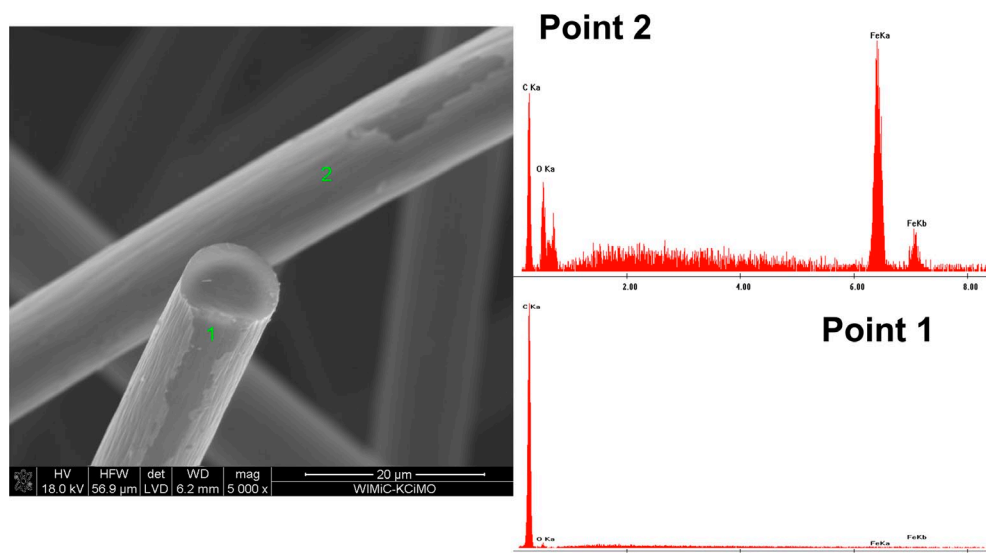


Fig. 2. Morphology of the surface of the trawls after magnetron iron coating for 10 minutes together with EDS analysis confirming the composition of the layer (point2) and fiber (point 1)

sputtering it is possible to change the surface character making it more hydrophobic (by a short deposition time) and lowering the wetting angle (by extending the deposition time).

The textural studies (BJH/BET) confirm that as the time of sputtering the fiber with iron increases, its surface becomes smoother. This fact is confirmed by the change in the size of the specific surface area, which for fibers sputtered for 2 minutes is  $37.4 \text{ m}^2/\text{g}$  (CF\_Fe2'), while for fibers sputtered for 10 minutes it is  $2.11 \text{ m}^2/\text{g}$  (CF\_Fe10'). Despite the 10-minutes iron deposition, the specific surface area of the modified fibers is still higher than that of the reference fibers (TABLE 2). These changes confirm the existence of an iron layer on the fibers, not only changing the nature of the surface (wettability, specific surface area), but especially a layer about 100 nm (SEM observation). The porosity of the carbon fibers does not change (~78-82%), regardless of the time of iron deposition on the fiber surface (2-10 min). The determined pore size (range: 50-100  $\mu\text{m}$ ) refers to the distance

TABLE 2

Characteristic textural parameters of CF\_Fe fibres

Samples	Shape factor, $d_1/d_2$	Pore size (inter-fibres diameter), $\mu\text{m}$	Porosity, %	BET surface area, $\text{m}^2/\text{g}$
CF	0.98	70-112	80.5	$0.55 \pm 0.05$
CF_Fe2'	0.98	60-85	82.4	$37.64 \pm 0.81$
CF_Fe4'	0.97	67-80	80.1	$21.64 \pm 0.45$
CF_Fe6'	0.95	69-98	79.3	$12.34 \pm 0.47$
CF_Fe8'	0.96	57-92	78.5	$5.26 \pm 0.21$
CF_Fe10'	0.96	54-98	78.2	$2.11 \pm 0.13$

between fibers. Neither micro nor mesopores were found on the fiber surface. The pore size distribution is unimodal. The average distance between fibers is 5% larger in the reference nonwoven compared to CF\_Fe2' and 3% larger than in CF\_Fe10'. Many authors working with ACF confirm that exceeding the limit value

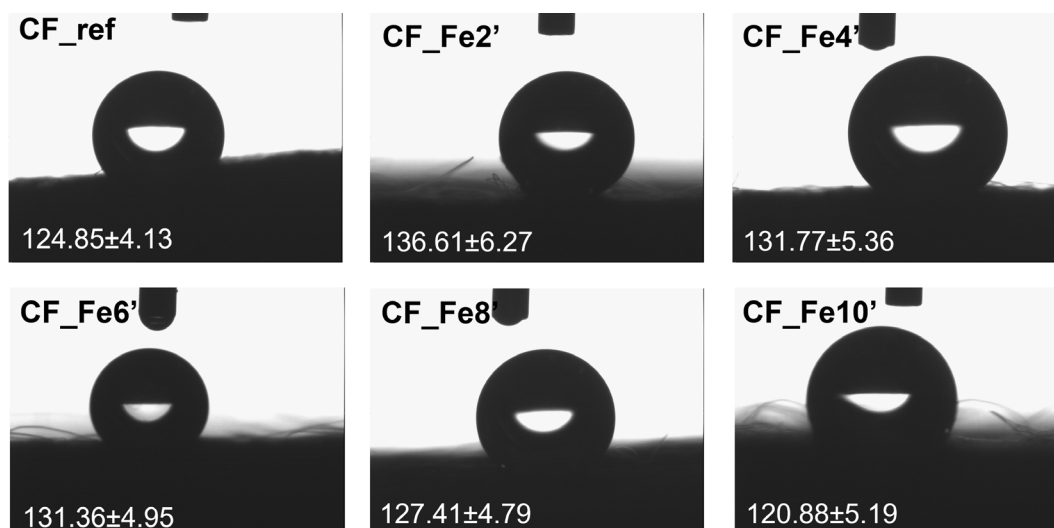


Fig. 3. Wettability of fiber surfaces determined for CF and CF\_Fe materials tested

of the modifier may destroy micro or mesopores by their collapse or/and expansion. As a result, the number of micropores and the specific surface area are usually reduced [18,19].

In the case of biocompatibility and surface-modified carbon fibre tests, the results of cytotoxicity and viability tests should be treated complementary [20]. A lot of information is also provided by staining which complements the knowledge about the active state of cells [21]. The cellular response improves due to changes in the surface chemistry caused by e.g. vaccination of protein compounds that facilitate cell adhesion [11]. As in the studied materials, cells are most willing to spread on surfaces

characterized by submicrometric or nanometric roughness and such surface chemistry that facilitates the formation of chemical interactions between the substrate and the cell membrane. All the studied iron-modified carbon fibers are biocompatible, as evidenced by the high osteoblast survival rates after 3 and 7 days of culture. With the increasing iron content, the cell viability rises and it is the highest for the CF\_Fe8' and CF\_Fe10' materials (Fig. 4a). Interestingly, the iron layer applied over a short period of time (CF\_Fe2', CF\_Fe4') slightly decreases the cell viability during the first culture period (3 days). Increasing the culture time accelerates the cell proliferation and after 7 days

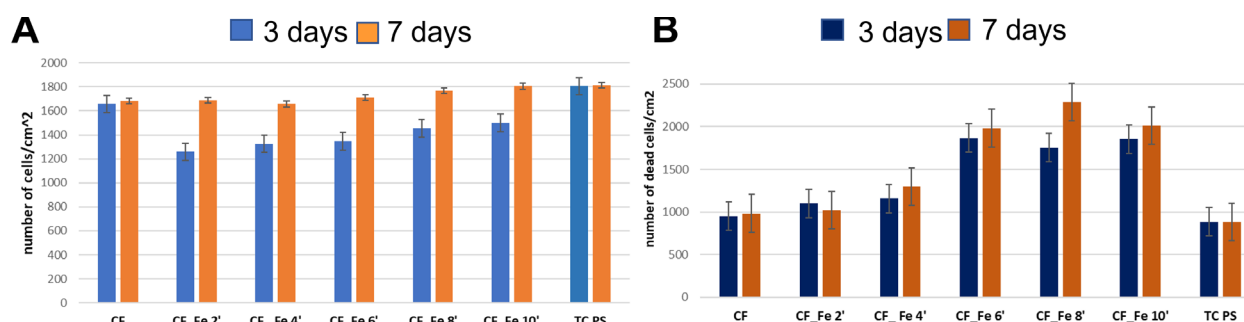


Fig. 4. Viability (A) and cytotoxicity (B) of MG-63 cells contacted with CF\_Fe materials and reference in the form of a nonwoven fabric composed of unmodified CF carbon fibers and cells contacted with the TCPS (tissue culture polystyrene)

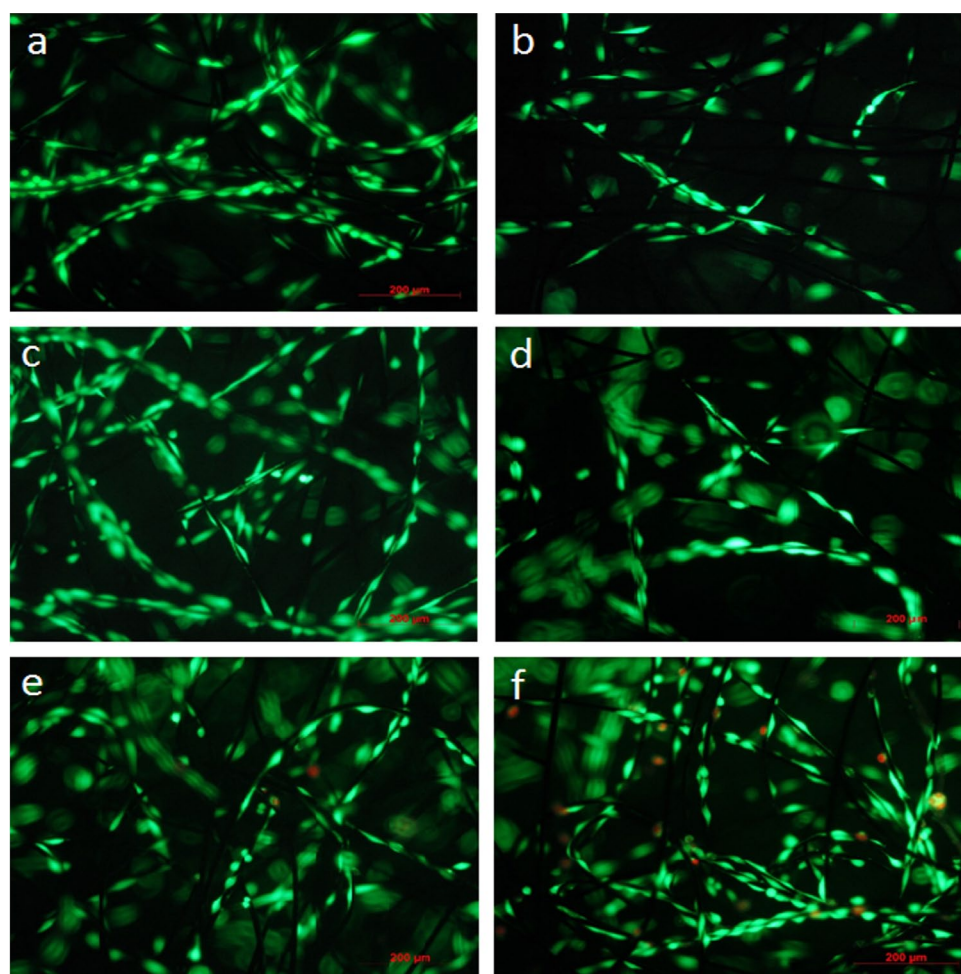


Fig. 5. Image of MG-63 cells after 3 days in *in vitro* conditions contacted with a reference materials CF (a) and CF after magnetron sputtering with iron CF\_Fe2' (b), CF\_Fe4' (c), CF\_Fe6' (d), CF\_Fe8' (e) and CF\_Fe10' (f). Images taken with a fluorescence microscope

the MG-63 cell viability is identical to that in the culture without the material (TCPS). The cell proliferation growth also rises the materials cytotoxicity (Fig. 4b). In the case of the nonwoven CF\_Fe2', the cytotoxicity is low, which may be influenced by this material's wettability value which is higher than the others' one. The rapid increase in the number of cells on the CF\_Fe8' and CF\_Fe10' materials may be the reason for the increased cytotoxicity. The cells from the first layers – directly in contact with the material – detach due to hypoxia and malnutrition. At the same time, the cells on the CF\_Fe2' and CF\_Fe4' materials are just starting to proliferate.

This suggestion is confirmed by the live-dead staining was performed on the cells contacted with the CF\_Fe2'-CF\_Fe10' materials (Fig. 5). For the CF\_Fe2, CF\_Fe4 and CF\_Fe6' materials, the correct morphology of osteoblasts spread along the fiber can be observed (Fig. 5b-d). For the CF\_Fe8' and CF\_Fe10' fibers, both living cells (green) and red spots are visible, confirming the presence of dead osteoblasts detached from the surface (Fig. 5f-e). It seems that the iron presence allows the formation of local contact adhesion point. This is supported by the correct morphology of cells but also by their high viability in the studied time. Longer sputtering time leads to the formation of a thicker layer of iron which can hinder cells adhesion or lead to detachment of the layer together with the adhered cells.

#### 4. Summary and conclusion

The research confirmed that the modified non-woven carbon fibre can be effectively coated with an iron layer in the thickness range of about 100 nm. The layer thickness depends on the exposure time – the longer it is (above 6 min), the more inhomogeneous the layer becomes and the more it cracks and falls off (based on the SEM observations). The surfacing process tidies up the fibre surface structure and affects its roughness. A short exposure time increases the surface development of the material, and as the exposure time increases, the surface becomes smoother (covered with a thicker homogeneous iron layer). The deposited iron layer is biocompatible with MG-63 cells. The use of the iron layer as a signal for magnetic resonance to control the tissue regeneration and simultaneous substrate degradation requires further studies.

To conclude: the magnetron method allows covering carbon fibers with a layer of iron; the quality of the layer affects the texture of the fiber surface and depends on the time of deposition, all the analyzed materials have a biocompatible nature, which allows us to think about their biomedical application

#### Acknowledgment

The work was supported by the National Science Center OPUS 16 UMO project 2018/31/B/ST8/02418.

#### REFERENCE

- [1] L. Qin, W.-F. Liu, X.-G. Liu, Y.-Z. Yang, L.-A. Zhang, *New Carbon Mater.* **35** (5), 459-485 (2020).
- [2] J.-S. Tsai, *J. Polym. Res.* **1** (4), 399-402 (1994).
- [3] Y.-C. Chiang, C.-C. Lee, H.-C. Lee, *J. Porous. Mater.* **14** (2), 227-237 (2007).
- [4] A. Sedghi, R.E. Farsani, A. Shokuhfar, *J. Mater. Proces. Tech.* **198** (1-3), 60-67 (2008).
- [5] A.-H. Lu, J.-T. Zheng, *J. Colloid Interface Sci.* **236** (2), 369-374 (2001).
- [6] H. Li, M. Liebscher, J. Yang, M. Davoodabadi, L. Li, Y. Du, B. Yang, S. Hempel, V. Mechtcherine, *J. Clean. Prod.* **368**, 133093 (2022).
- [7] H. Li, M. Liebscher, I. Curosu, S. Choudhury, S. Hempel, M. Davoodabadi, *Cem. Concr. Compos.* **114**, 103777 (2020).
- [8] M.F. Hassan, M.A. Sabri, H. Fazal, A. Hafeez, N. Shezad, M. Husain, *J. Anal. Appl. Pyrolysis.* **145**, 104715 (2020).
- [9] T. Weigel, J. Brennecke, J. Hansmann, *Mater.* **12** (6), 1378 (2021).
- [10] O.K. Alexeeva, V.N. Fateev, *Int. J. Hydrogen Energy* **41** (5), 3373-3386 (2016).
- [11] J. Frączyk, S. Magdziarz, E. Stodolak-Zych, E. Dzierzkowska, D. Puchowicz, I. Kamińska, M. Giełdowska, M. Boguń, *Mater.* **14** (12), 3198 (2021).
- [12] Lonza, ViaLight plus kit cell viability assay, 1-5 (2011).
- [13] Lonza, ToxiLight™ bioassay kit, 3-7 (2011).
- [14] S.M. Manocha, H. Patel, L.M. Manocha, *J. Mater. Eng. Perform.* **22** (2), 396-404 (2013).
- [15] J.R. Naik, M. Bikshapathi, R.K. Singh, A. Sharma, N. Verma, H.C. Joshi, A. Srivastava, *Environ. Eng. Sci.* **28** (12), 725-733 (2011).
- [16] A.A. Lysenko, *Fiber Chem.* **39**, 93-102 (2007).
- [17] Y. Kohgo, K. Ikuta, T. Ohtake, Y. Torimoto, J. Kato, *Int. J. Hematol.* **88** (1), 7-15 (2008).
- [18] Q. Zuo, H. Zheng, P. Zhang, Y. Zhang, *Langmuir.* **38** (1), 253-263 (2022).
- [19] A. Tabet-Aoul, M. Mohamedi, *Phys. Chem.* **14**, 4463e74 (2012).
- [20] Ł. Zych, A.M. Osyczka, A. Łacz, A. Różycka, W. Niemiec, A. Rapacz-Kmita, E. Dzierzkowska, E. Stodolak-Zych, *Mater.* **14** (4), 843 (2021).
- [21] E. Stodolak-Zych, P. Jeleń, E. Dzierzkowska, M. Krok-Borkowicz, Ł. Zych, M. Boguń, A. Rapacz-Kmita, B. Kolesińska, *J. Mol. Struc.* 1211, 128061 (2020).